Progress in Organic Coatings 185 (2023) 107942

Contents lists available at ScienceDirect

Progress in Organic Coatings

journal homepage: www.elsevier.com/locate/porgcoat

Easy-to-prepare graphene-based inkjet-printed electrodes for diclofenac electrochemical sensing

Daria Minta [a], Zoraida González [b,*], Sonia Melendi-Espina [c], Grażyna Gryglewicz [a,*]

[a] Department of Process Engineering and Technology of Polymer and Carbon Materials, Faculty of Chemistry, Wrocław University of Science and Technology, Gdańska 7/9, 50-344 Wrocław, Poland
[b] Instituto de Ciencia y Tecnología del Carbono (INCAR), CSIC, Francisco Pintado Fe 26, Oviedo 33011, Spain
[c] School of Engineering, University of East Anglia, Norwich Research Park, Norwich NR4 7TJ, United Kingdom

ARTICLE INFO

Keywords:
Graphene oxide-based inks
Inkjet-printing technology
Post-processing thermal treatments
Water contaminants of emerging concern
Cutting edge electrochemical sensors

ABSTRACT

Inkjet-printed electrodes (IPEs) from flexible Kapton® as substrate and easy to prepare graphene oxide (GO)-based inks (K/GO) were prepared using a standard desktop printer. Subsequently, they were submitted to a post-processing thermal treatment (K/GO_TR400) and assessed as disposable working electrodes (WEs) for diclofenac (DCF) indirect electrochemical detection at pH 7.0 (close to physiological pH value). DCF monitoring is attracting much interest, due to its classification as contaminant of emerging concern in water sources. The performance of the printed active sensor material was compared to that of thermally reduced (at 400 °C) graphene oxide (TRGO-400, in a powder form), which has been successfully used as glassy carbon electrode (GCE) modifier for the detection of DCF. This electrode worked linearly within the concentration range between 5 and 25 μM with an LOD value of 2.25 μM. Moreover, the morphology and chemical composition of the obtained IPEs were characterized by means of scanning electron microscopy (SEM) and X-ray photoelectron spectroscopy (XPS) and compared with GCE/TRGO-400. Cyclic voltammetry (CV) and differential pulse voltammetry (DPV) measurements using a miniaturized 3-electrode cell of the post-processed IPEs showed a promising electrochemical performance for DCF sensing. Thus, this study demonstrated the effective partial recovery of the valuable properties of graphene on the IPEs after the thermal treatment and the successful production of flexible and disposable electrodes for target analyte detection. Therefore, this is a promising alternative to conventional modified GCEs, as it offers a facile approach for the fabrication of cutting edge graphene-based electrodes and widens the available portfolio of electrochemical sensors towards detection of water contaminants of emerging concern.

1. Introduction

Diclofenac (DCF), an active substance in commercially available drugs (Acoflam, Diclac, Monoflam and Voltaren), has been widely used to treat several diseases affecting humans, such as pneumonia and inflammation. Interest in monitoring pharmaceuticals, including DCF, in water sources has markedly increased in recent years because of their low biodegradation in the environment, which has negative consequences for animals and ecosystems [1,2]. Therefore, DCF has been prioritized as a water contaminant of emerging concern, i.e., a chemical that is not currently or has only recently started to be regulated and that poses a concern regarding its impact on human or ecological health [3]. Therefore, it is necessary to design and develop appropriate procedures for the detection of this compound and prevent it from becoming a persistent pollutant [4]. Traditionally, analytical methods (such as potentiometry, spectroscopy and chromatography) have been the most used methods for detecting DCF [2]. However, these procedures are time-consuming, expensive and experimentally complex, thus motivating the scientific community to seek alternative sensing methodologies [5,6].

In recent years, electrochemical sensors have gained significant interest to overcome the previously mentioned drawbacks. Electrochemical sensors are characterized by their short analysis time, high selectivity and sensitivity, absence of complex sample pre-treatments and the possibility of automatization. Thus, they are promising alternatives to reliable qualitative and/or quantitative determination of DCF

* Corresponding authors.
E-mail addresses: zoraidag@incar.csic.es (Z. González), grazyna.gryglewicz@pwr.edu.pl (G. Gryglewicz).

https://doi.org/10.1016/j.porgcoat.2023.107942
Received 8 June 2023; Received in revised form 23 August 2023; Accepted 1 September 2023
Available online 14 September 2023
0300-9440/© 2023 The Authors. Published by Elsevier B.V. This is an open access article under the CC BY license (http://creativecommons.org/licenses/by/4.0/).

[7]. However, conventional bare electrodes (i.e., glassy carbon, carbon paste, and screen-printed electrodes) exhibit poor electrochemical behavior in the redox processes of interest. Consequently, bare electrodes need to be modified with active materials to improve their performance towards the detection of the target analyte.

In this context, special attention has been paid to the use of graphene-based materials as electrode modifiers in the fabrication of electrochemical sensors. Considering their easy and scalable synthesis, relatively high electrical conductivity and tunable surface chemistry, graphene materials are suitable for the determination of a wide range of analytes [8,9]. However, there are also disadvantages associated with the use of these sensors, mainly related to the homogeneous distribution of the modifier on either the glassy carbon electrode (GCE) or the screen-printed carbon electrode (SPCEs) surface.

Therefore, to take a step forward in the design, development, and manufacture of a novel concept of point-of-care electrochemical sensors for DCF detection, inkjet printing technology appears to be a very promising alternative [10]. Graphene-based inkjet-printed electrodes (IPEs) are currently being explored by the scientific community, paying special attention to the development of appropriate functional inks, patterns and post-printing treatments aimed at obtaining appropriate sensing platforms for target analytes.

Pandhi et al. [11] proposed a fully inkjet-printed multi-layered graphene (MLG) electrode for the ferric/ferrocyanide redox couple. A mixture of graphite/ethanol/ethyl cellulose was sonicated to obtain a graphene-based ink printed onto a Kapton substrate using a Dimatix IJP printer (Fujifilm). The detection limit (LOD) obtained for the redox processes of interest was 0.01 mM.

To improve the application potential of the proposed electrodes, research on inkjet printing has focused on complex ink formulations containing conductive polymers or metallic nanoparticles. Nevertheless, the printing of complex inks can lead to several disadvantages concerning the final properties of printed films, such as their lack of homogeneity and low long-term stability. Inkjet-printed graphene-poly (3,4-ethylenedioxythiophene):poly(styrene-sulfonate) (PEDOT:PSS) printed on SPCEs using a Fujifilm Dimatix Materials Printer was used as a salbutamol (SAL) electrochemical detection platform. The obtained sensor worked linearly between 5 and 550 μM presenting a limit of SAL detection of 1.25 μM [12]. A complex nanosilver-decorated graphene/cyclohexanone/terpineol-based water ink, proposed by Deng et al. [13], was printed on polyimide using a Microfab Jetlab4 printing system (Microdrop Technologies GmbH, Germany). The proposed platform has not yet been tested in any application. However, owing to its excellent conductivity and flexibility, it is promising for printed electronics, particularly as electrode.

In this study, the preparation of GO-based inkjet-printed electrochemical sensors for DCF sensing was assessed as a novel, facile and straightforward approach to replace conventionally used modified GCEs. Starting with water-based GO suspensions, the formulation of suitable inks for subsequent printing was optimised by evaluating different surfactants and using carbon black as a conductive additive. Subsequently, Kapton was selected as a flexible substrate, followed by a sustainable and scalable post-processing thermal treatment, to successfully develop disposable and miniaturized sensing platforms for target analytes.

The physicochemical characteristics of the as-prepared IPEs were comparable to those of the TRGO-400 powder (graphene material produced by thermal exfoliation and reduction of graphite oxide) used as a GCE modifier. The electrochemical characterization of the IPEs for DCF detection showed promising results, encouraging to improve graphene-based inks and IPEs processing to obtain improved sensing platforms, thus widening the scope of available electrochemical sensors for several water contaminants of emerging concern.

2. Experimental section

2.1. Preparation of graphene-based materials

Graphite oxide (GrO) was obtained by the oxidative treatment of commercial graphite as starting material (synthetic graphite powder, particle size <70 μm, from Sigma-Aldrich) using a modified Hummers method [14]. Subsequently, to obtain GO–water suspensions at different concentrations (4000, 7000 and 9000 ppm) previously obtained GrO was submitted to sonication for 8 h.

For comparative purposes, TRGO-400 powder for conventional GCE modification was prepared starting from the same GrO, which was subjected to a one-step thermal exfoliation/reduction protocol, as described elsewhere [15].

2.2. Preparation of GO-based inks

As previously mentioned, three different concentrations of water-based GO suspensions were selected as raw materials (GO-X, X = 4000, 7000 and 9000 ppm) to obtain inks suitable for subsequent printing. In the second step, two surfactants were evaluated to achieve the appropriate stability of the inks. Triton X-100 (GO-X_TX) and sodium dodecyl sulphate (GO-X_SDS) were added to the GO suspensions in a 2:1 (*w*/w) ratio. Finally, 10 mg of carbon black (CB - VULCAN® XC72 carbon black, CABOT, CB:GO = 1:35 w/w) were added to selected ink formulations as conductive additive (GO-X_S_CB, S being tested surfactant).

2.3. Preparation of graphene-based sensing platforms

The IPEs were manufactured using a commercial inexpensive EPSON EcoTank ET-M2120 desktop printer. Kapton (DuPontTM Kapton®) was selected as the most suitable substrate owing to its high thermal stability (up to 450 °C) and thus bearing in mind the post-printing procedure under consideration. Before use, the printer cartridge was cleaned several times with ultrapure water to remove any residual ink. All tested inks were homogenised for 10 min at 2000 rpm using a SpeedMixer (German Engineering by Hauschild, type DAC 150.1 FVZ-K) and filtered using 0.45-μm syringe filter before being introduced into the printer cartridge (avoiding the formation of bubbles). Printing patterns were designed using the EPSON software by varying the number of printed GO-based layers, thus obtaining IPEs from different GO concentrations but also with dissimilar thicknesses (K/GO-X_S_CB_Y, where Y is the number of printed layers, from 7 to 10). After printing, selected IPEs were submitted to a post-processing thermal treatment in an inert atmosphere (400 °C, 1 h, 200 mL min^{-1} N_2 flow). The resulting electrodes were labelled as K/GO-X_S_CB_Y_TR400. Silver ink was applied to ensure appropriate electrical contact between the as-obtained WEs and the potentiostat used to perform electrochemical characterization measurements.

For comparison, traditional modified GCEs were also prepared. First, GCEs were polished with alumina oxide and washed with Milli-Q water. Then, cleaned electrodes were modified with 2.5 μL of a dispersion that was prepared by mixing 4 mg of TRGO-400 powder and 1 mL of dimethylformamide (DMF, Sigma Aldrich, Saint Louis, USA)/Milli-Q water solution (ratio of 1:1 v/v) followed by sonication for 3 h. Subsequently, the electrodes were dried under an infrared lamp before use. The prepared electrodes were labelled as GCE/TRGO-400.

2.4. Preparation of artificial urine samples

Artificial urine (AU) solution was prepared following a protocol proposed by Chutipongtanate and Thingboonkerd and proposed as real sample [16]. The artificial urine was prepared by dissolving 2.427 g urea, 0.034 g uric acid, 0.900 g creatinine, 0.297 g $Na_3C_6H_5O_7{\cdot}2H_2O$, 0.634 g NaCl, 0.450 g KCl, 0.161 g NH_4Cl, 0.089 g $CaCl_2{\cdot}2H_2O$, 0.100 g

$MgSO_4 \cdot 7H_2O$, 0.034 g $NaHCO_3$, 0.003 g NaC_2O_4, 0.258 g Na_2SO_4, 0.100 g $NaH_2PO_4 \cdot H_2O$ and 0.011 g Na_2HPO_4 in 200 mL of Milli-Q water.

2.5. Characterization of the materials

The morphology of different IPEs, before and after thermal treatment, and TRGO-400 powder (as GCE modifier) was examined by means of scanning electron microscopy (SEM, MERLIN Zeiss with EDS X-Flash®5010 Bruker Nano detector). The surface chemistry of the materials was determined by X-ray photoelectron spectroscopy (XPS) analysis using a VG-Microtech Multilab 3000 spectrometer (SPECS, Germany) equipped with a hemispherical electron analyzer and a MgKα ($h\nu = 1253.6$ eV) X-ray source. The type of carbon bonding and the oxygen functional groups in the samples were estimated by curve fitting the C1s spectra using a Gaussian–Lorentzian peak shape after performing a Shirley background correction. The XPS spectra were calibrated with respect to the C1s signal at a binding energy of 284.5 eV. In addition, the electrical resistance of the inkjet-printed sensing platforms was evaluated using the four-point methodology (Jandel RM3000+ test unit attached to a Jandel cylindrical four-point probe head - Jandel Engineering, Leighton Buzzard, UK) [17,18].

2.6. Electrochemical measurements

The electrochemical performance of the selected IPEs for DCF detection was tested in a lab-made miniaturized electrochemical cell in which the IPEs acted as WEs. A micro-Ag/AgCl electrode and a graphite rod were used as the reference (RE) and counter (CE) electrodes, respectively (Fig. 1).

In parallel, as previously mentioned, the GCE modified with TRGO-400 was electrochemically characterized in a lab-designed three-electrode cell using Ag/AgCl/3.5 M KCl (i.e., 0.205 V vs. NHE) as the RE and a graphite rod as the CE. In all cases, cyclic voltammetry (CV) measurements (potential range: −0.3 to 1.0 V, scan rate: $\nu_{scan} = 50$ mV s^{-1}) were performed using 0.1 M phosphate-buffer saline solution (PBS) containing 100 μM DCF as the electrolyte (pH = 7.0). To determine the electrochemical behavior of the sensor, differential pulsed voltammetry (DPV) was performed after optimising the experimental parameters (t = 20 s, $P_H = 100$ mV, $P_W = 25$ ms, and $S_T = 75$ mV). Furthermore, to gain insight into the post-processing thermal treatment performed on GO-based IPEs, EIS measurements were carried out (in a 0.1 M PBS solution, pH = 7.0 containing 10 mM of $[Fe(CN)_6]^{3-/4-}$) at frequencies from 0.1 to 10^2 kHz using a DC potential of 0.25 V.

3. Results and discussion

3.1. Materials characterization

Fig. 2 presents, as an example, the morphology of selected IPEs, before and after post-processing by thermal treatment at 400 °C (K/GO-7000_TX_CB_8 and K/GO-7000_TX_CB_8_TR400). Criteria for this selection are explained in detail in the next section. For comparative purposes, an image corresponding to TRGO-400 powder used as GCE modifier was also included. It is determined that IPEs made from graphene-based materials (Fig. 2(a) and (b)) display a smooth and homogenous coverage of the Kapton substrate. Moreover, aggregates resulting from the presence of carbon black are noticed, thus corroborating the successful incorporation of this conductive additive into the ink formulation [19]. As previously reported, TRGO-400 powder showed an aggregated structure of wrinkled graphene sheets (Fig. 2c). Several accordion-type structures are clearly visible, which means that TRGO-400 is not fully exfoliated [20,21].

To gain insight into the surface chemistry of the proposed sensing platforms, XPS analysis was performed. According to the results summarised in Table 1, the oxygen content of K/GO-7000_TX_CB_8 (31.1 at. %) is markedly higher than that measured on K/GO-7000_TX_CB_8_TR400 (9.1 at. %) confirming the successful removal of oxygenated functional groups when submitting the starting GO-based IPE to the post-processing thermal treatment at 400 °C. Furthermore, the degree of achieved reduction was comparable to that of the TRGO-400 powder (O = 10.1 at. %) proving the feasibility of the post-processing procedure on inkjet-printed films.

More detailed information on the type and distribution of the oxygenated functional groups present in the active electrode materials under evaluation was obtained after deconvolution of the corresponding XPS C1s core-level spectra (Fig. 3).

The C1s core-level spectra of K/GO-7000_TX_CB_8, K/GO-7000_TX_CB_8_TR400 and TRGO-400 were deconvoluted into five components: C sp^2 (284.5 eV), Csp^3 (285.4 eV), hydroxyl and epoxy groups (286.5 eV), carbonyl and quinone groups (287.6 eV), and lactone and carboxylic groups (289.0 eV) [22]. As shown in Table 2, after thermal treatment, the obtained active materials (K/GO-7000_TX_CB_8_TR400 and TRGO-400) exhibited a high contribution of Csp^2 carbon, which is in agreement with previously reported studies, and demonstrate the successful reduction of the starting GO [23]. Thus, after the thermal treatment of K/GO-7000_TX_CB_8, the contribution of the hydroxyl and epoxy groups significantly decreases from 49.0 % to 13.2 %. The slight increase in the contribution of the carboxyl/lactone

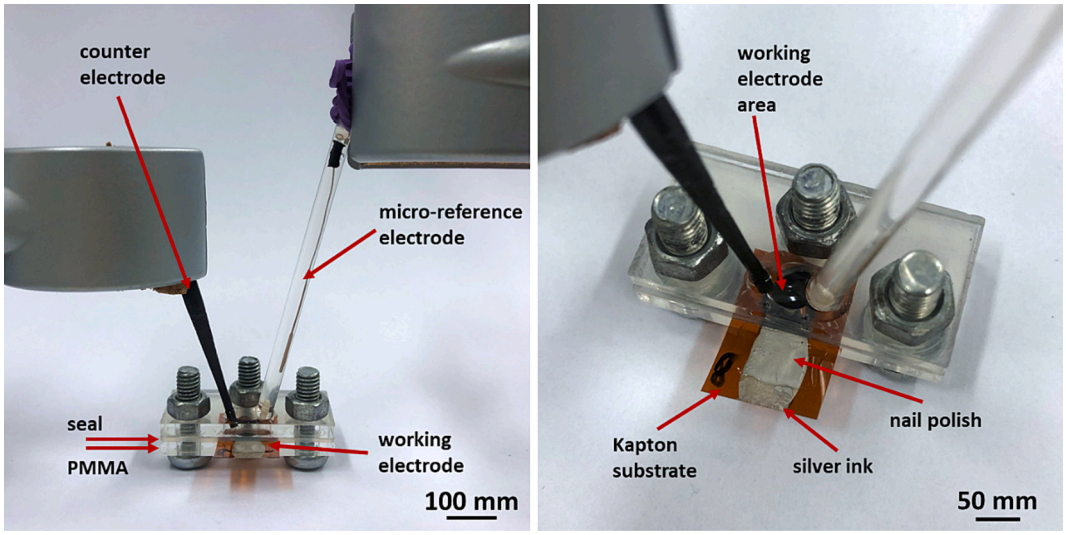

Fig. 1. Miniaturized 3-electrodes electrochemical setup using IPEs as WEs.

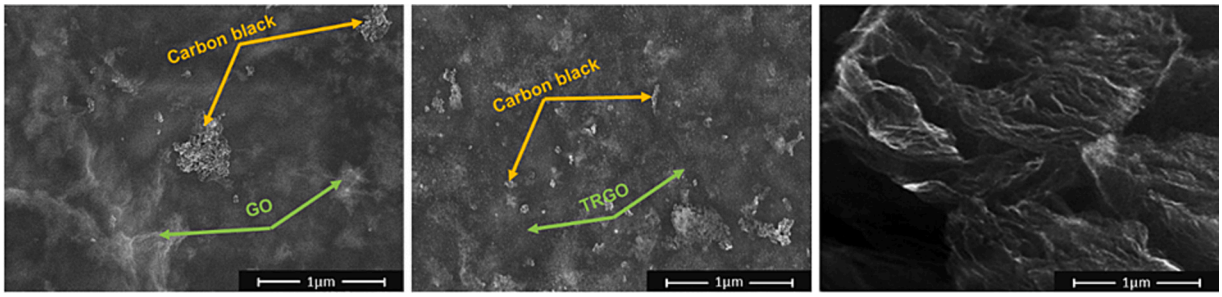

Fig. 2. SEM pictures of (a) K/GO-7000_TX_CB_8, (b) K/GO-7000_TX_CB_8_TR400 and (c) TRGO-400.

Table 1
Chemical surface composition of the sensing platforms under evaluation (at. %).

Sample	C	O
K/GO-7000_TX_CB_8	68.7	31.3
K/GO-7000_TX_CB_8_TR400	90.9	9.1
TRGO-400 powder	89.9	10.1

peak can be explained by the conversion of less stable oxygen groups into lactone moieties [24,25]. The similar surface chemistry of the K/GO-7000_TX_CB_8_TR400 and TRGO-400 powder clearly indicates the successful reduction of the active electrode material printed on Kapton.

Electrical conductivity measurements were performed on the selected IPEs. A marked decrease of sheet resistance was observed after addition of CB (3.96 vs. 5.10 kΩ $sq.^{-1}$ for K/GO-7000_TX_CB_8_TR400 and K/GO-7000_TX_8_TR400, respectively). As expected, the sheet resistance of K/GO-7000_TX_CB_8 was markedly higher (giving values close to isolating material). Moreover, EIS measurements were also performed to evaluate the behavior of IPEs before/after thermal treatment towards the electron transfer involved in a faradaic process. Thus, Fig. S2 (Supporting Information) shows the Nyquist plots recorded on the tested electrodes using $[Fe(CN)_6]^{3-/4-}$ as the redox probe. According to literature, the diameter of the semicircle recorded in the high frequency range is proportional to the charge transfer resistance of the electrode [26]. After the thermal treatment the semicircle diameter significantly decreased which indicates the successful reduction of starting GO, thus improving the electron transfer and corroborating the high electrical conductivity of resulting IPE.

3.2. Electrochemical measurements

3.2.1. Electrochemical performance of IPEs after thermal post-processing for DCF detection

3.2.1.1. Optimization of GO-based ink formulation. The performance of the manufactured IPEs in DCF sensing was assessed by electrochemical measurements performed in a miniaturized cell, as previously described (Fig. 1, Experimental Section). DCF electrochemical sensing is a complex process encompassing several steps and side reactions (Fig. 4).

According to the literature, DCF is first oxidized at a potential close to 0.6 V vs. Ag/AgCl (peak I). The resulting product is chemically decomposed into 2,6-dichloroaniline and 2,2-hydroxyphenyl acetic acid. In the second electrochemical step, the latter compound is first reduced to 1-hydroxy-2-(hydroxyphenyl)ethanalate and reversibly oxidized (peak II) at potential values of 0.30 and 0.35 V, respectively [26]. Most studies focused on the first electrochemical reaction of DCF (peak I). In contrast, Aquilar-Lira et al. [26] compared the suitability of this detection procedure with that used for the oxidation of 1-hydroxy-2-(hydroxyphenyl) ethanalate. According to their results, significantly improved sensor working parameters were obtained when using the latter redox reaction. This, together with the chemical instability of oxidized DCF, led us to focus on the indirect detection of DCF through the oxidation of 1-hydroxy-2-(hydroxyphenyl) ethanalate.

Table 2
Results of C1s spectra deconvolution (%).

Sample	C1s peak deconvolution				
	Csp^2	Csp^3	C-OH	C=O	O=C-OH
K/GO-7000_TX_CB_8	42.5	12.1	32.9	7.1	5.4
K/GO-7000_TX_CB_8_TR400	60.9	16.6	13.2	4.3	5.0
TRGO-400 powder	60.5	16.7	11.8	6.1	4.9

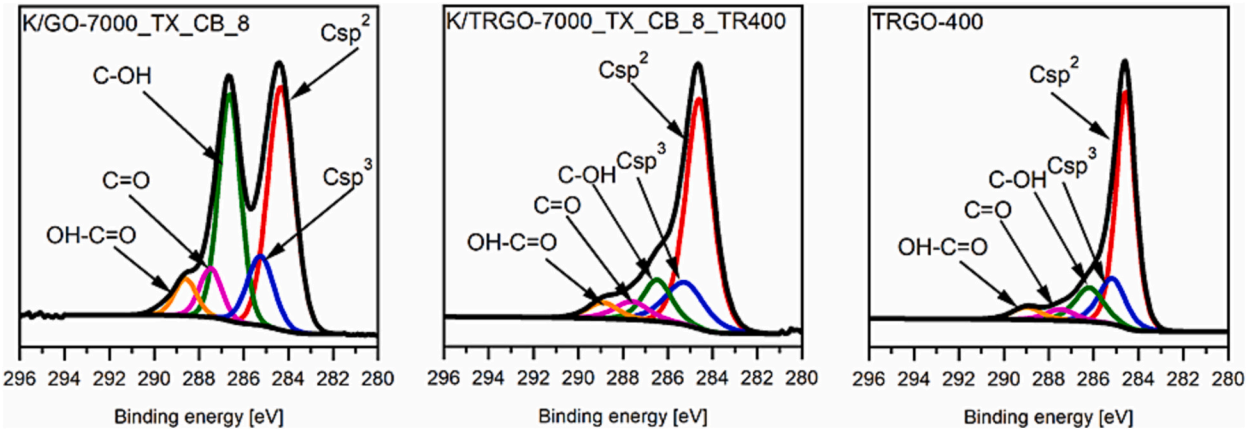

Fig. 3. Deconvolution of the C1s core-level spectra of the materials.

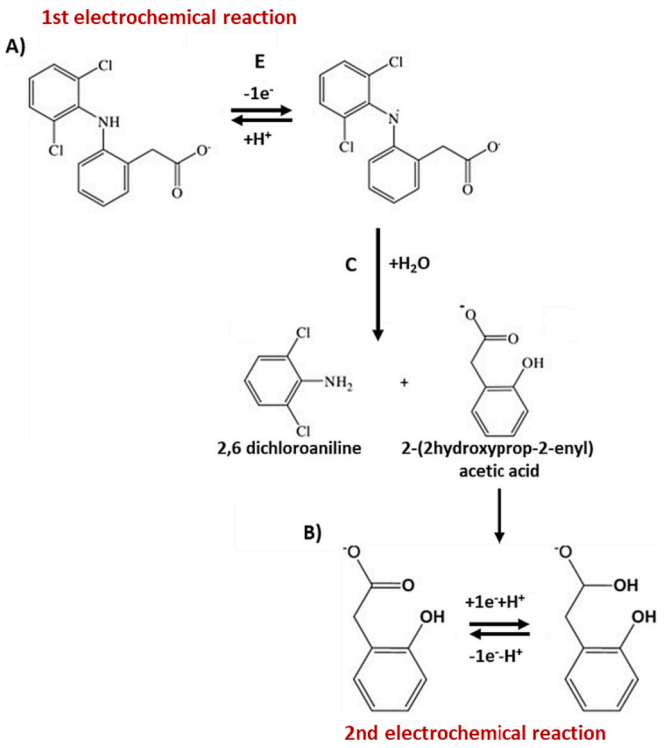

Fig. 4. (A) Mechanism of the main DCF anion electrochemical oxidation reaction in aqueous medium at pH 7. (B) Mechanism of the non-direct electrochemical detection of DCF by faradaic process of the by-product 2-(2hydroxyprop-2-enyl) acetic acid. Reproduced with permission from [26].

Fig. 4(a–c) show the preliminary CV results regarding the electrochemical behavior for DCF sensing of a range of IPEs. As previously mentioned, the tested IPEs were manufactured by varying formulation of inks and experimental processing parameters (X – GO concentration, S – selected surfactant and Y – number of printed layers), using the same amount of conductive additive (CB – carbon black), and applying the same post-printing thermal treatment (400 °C, 1 h).

In the first stage, the concentration of GO used to prepare the water-based inks for inkjet printing was optimised (Fig. 5a). With this aim, GO suspensions with increasing concentrations (4000, 7000 and 9000 ppm) were prepared, and a fixed number of graphene-based layers (eight) were printed. The tested IPEs exhibited comparable results based on the measured capacitive currents. Nevertheless, the anodic peak currents ascribed to the DCF Faradaic process of interest clearly differ, being significantly lower when K/GO-4000_TX_8_TR400 was used as the sensing platform. Moreover, the overpotential of the anodic process is higher for this electrode. These results can be explained by the lack of homogeneity of this inkjet-printed graphene-based film because of the low concentration of the active material, which may negatively impact the electrical conductivity of the electrode. However, the CVs recorded for the IPEs printed using GO suspensions with higher concentrations were nearly identical; therefore, GO at a concentration of 7000 ppm was selected as the optimum concentration for formulating the required inks.

In the second stage, the addition of different surfactants to the GO-based ink formulation was assessed to gain insight into their role in improving the adhesion of the active film to the Kapton substrate, mainly after post-processing thermal treatment. Triton X-100 and SDS were added to the GO-7000 aqueous suspension at a weight ratio of 2:1. As shown in Fig. 5b, the electrodes printed from the GO-based ink incorporating Triton X-100 as a surfactant perform more efficiently because the DCF anodic currents are higher than those measured on electrodes containing SDS. This improved result can be explained by the better suitability of Triton X-100 surfactant as ink stabiliser and its lower negative impact on the electrical conductivity of the active electrode material.

In all cases, carbon black was added as a conductive additive to enhance the electrical conductivity of the resulting printed active films. As shown in Fig. 5c, the addition of carbon black resulted in the development of a specific surface area of the electrode, as the capacitive currents increases. Moreover, the oxidation peak potential shifts towards lower values, which indicates an enhancement of electron transfer on the electrodes incorporating CB, thus corroborating previous sheet resistance measurements.

Another parameter that requires optimisation during inkjet printing is the number of graphene-based layers in the printed patterns; this parameter is key to achieving homogeneous coverage of the substrate (avoiding defects and/or breaks) and use the least possible amount of active material. Thus, four different numbers of printed layers (from seven to ten) were prepared.

Considering peak II (previously selected to assess DCF indirect oxidation process), IPEs manufactured by printing 8–9 layers show higher anodic currents Fig. 5d and e. However, IPE with 9 layers of active material also displays a higher capacitive current. Thus, and considering the least amount of ink needed, IPE from 8 layers was selected as the most suitable one.

In addition, pictures showing the quality of previously described and characterized IPEs are shown in Fig. 5f. As it can be seen when printing >8 layers of the GO-based ink some smears are visible (marked with arrows), being this result an additional proof of film unsuitability for its use as sensing platform.

3.2.2. *Preliminary DCF sensing performance of IPEs in comparison with conventionally modified GCEs*

The peak corresponding to the reduction of 2,2-hydroxyphenyl acetic acid is also properly developed. It is clearly visible that post-processing thermal treatment has a remarkable positive influence on the electrochemical performance of the resulting electrode towards DCF electrochemical detection. No peaks were recorded on the starting electrode material (K/GO-7000_TX_CB_8) (Fig. 6a).

For comparative purposes CVs recorded on GCE/GO and GCE/TRGO-400 electrodes are also displayed (Fig. 6b). The response towards DCF is negligible on materials before thermal treatment. According to the obtained results, the capacitive current recorded on modified GCE/TRGO-400 is higher than that measured on K/GO-7000_TX_CB_8_TR400, which is in agreement with the lower surface area of the thinner and homogeneous layer of active material in the IPE. However, faradaic peaks corresponding to DCF redox processes are evidently distinguishable on both electrodes.

In Fig. 7a, the baseline corrected DPVs recorded on the selected IPE are presented. As it can be seen, the peak ascribed to the DCF sensing is highly distinctive, even though being quite broad. This could be explained by the overlapping of the two anodic peaks related to DCF oxidation processes (the direct one and that corresponding to the side reaction of 1-hydroxy-2-(hydroxyphenyl) ethanalate). At this point it is important to highlight that the main oxidation process of DCF (at 0.6 V) displays a lower faradaic current than the indirect one (at 0.35 V), thus verifying the low stability of the compound resulting from direct DCF oxidation and promoting the indirect DCF sensing process. For comparative purposes the baseline corrected DPV recorded on GCE/TRGO-400 is shown in Fig. 7b. On this electrode, peaks attributed to DCF redox processes are well developed and resolved. Corresponding DPVs and calibration curve were also determined on GCE/TRGO-400 electrode (Fig. 7c and d). This sensor works linearly between 5 and 25 μM with a LOD of 2.25 μM. It must be underlined that data recorded on K/GO-7000_TX_CB_8_TR400 are considered as preliminary results. However, they provide a promising insight to the indirect electrochemical detection of DCF at pH 7.0 using a new miniaturized electrochemical setup. Consequently, the obtained results are the first step of a novel approach for the preparation of electrochemical sensors and may

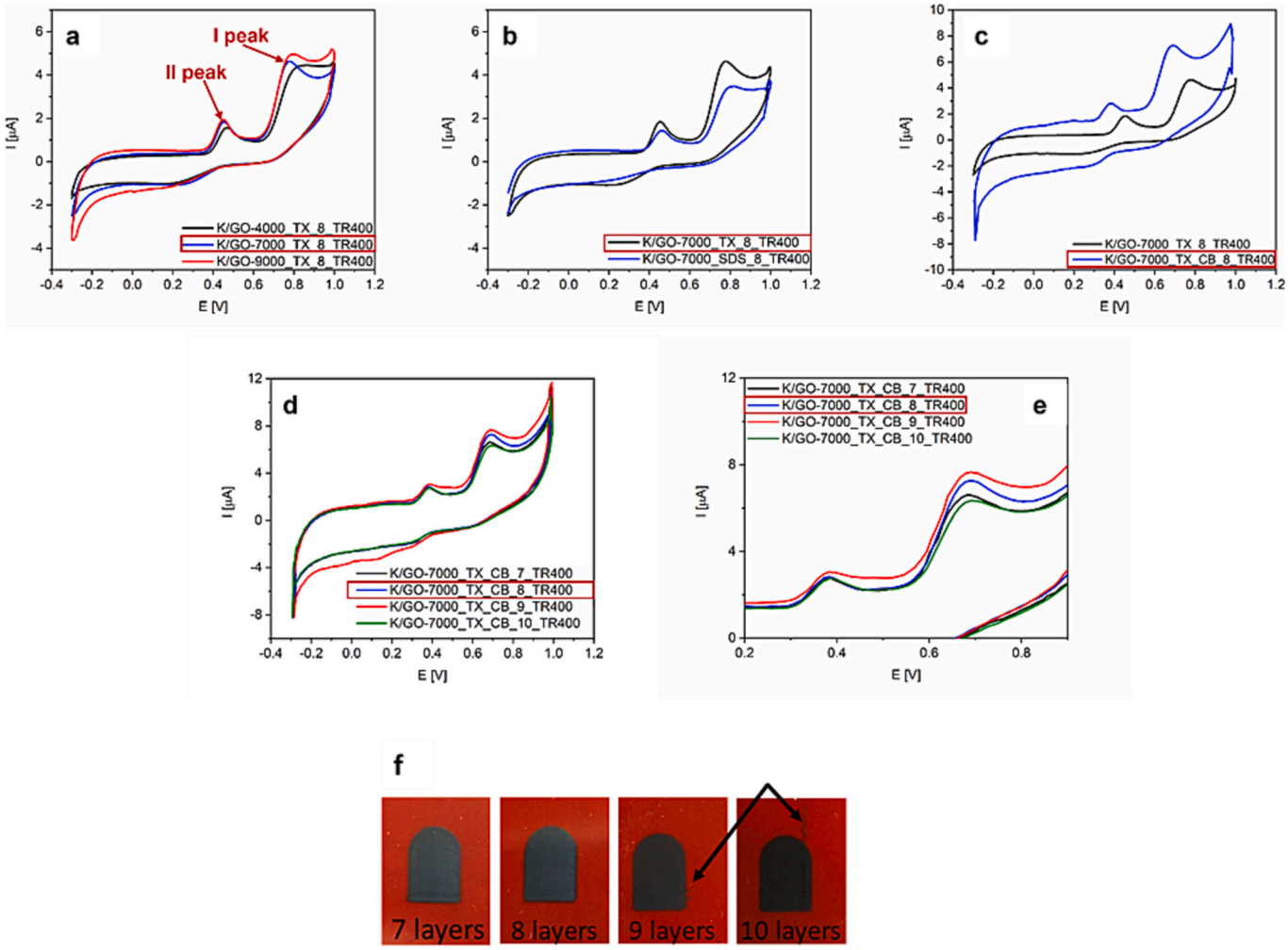

Fig. 5. (a-e) CVs recorded on K/GO-X_S_CB_Y_TR400 electrodes manufactured using different GO-based inks formulations. A 0.1 M PBS solution (pH 7.0) containing 100 µM DCF was used as electrolyte. (f) Pictures of K/GO-7000_TX_CB_Y_TR400 electrodes differing in the number of GO-based printed layers (from 7 to 10).

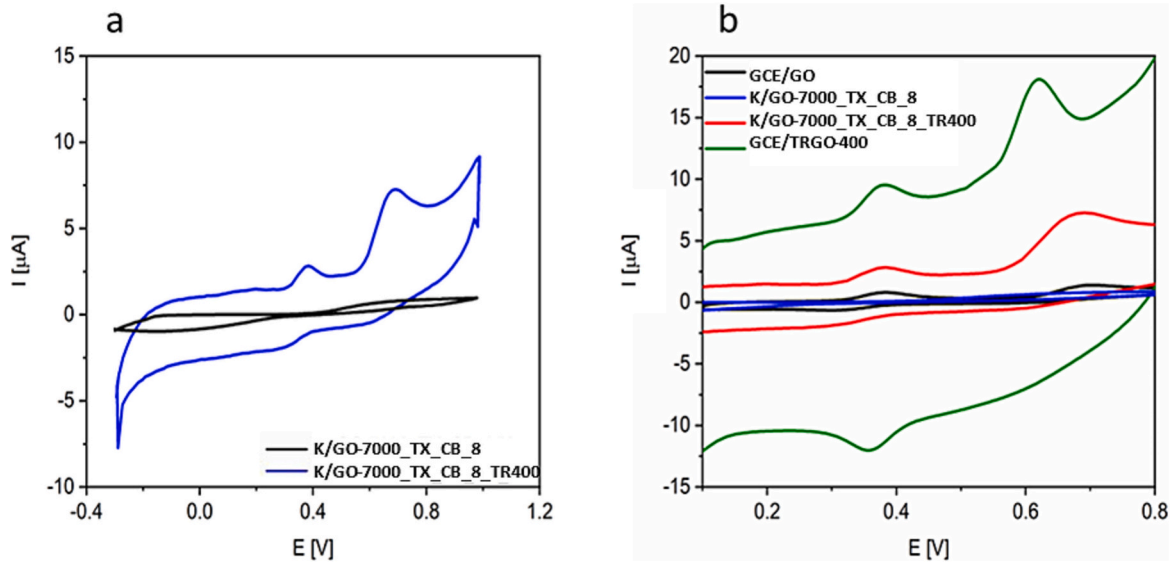

Fig. 6. CVs recorded on (a) K/GO-7000_TX_CB_8 and K/GO-7000_TX_CB_8_TR400 sensors. (b) Comparison with GCE/GO and GCE/TRGO-400 conventional electrodes. A 0.1 M PBS solution (pH 7.0) containing 100 µM DCF was used as electrolyte.

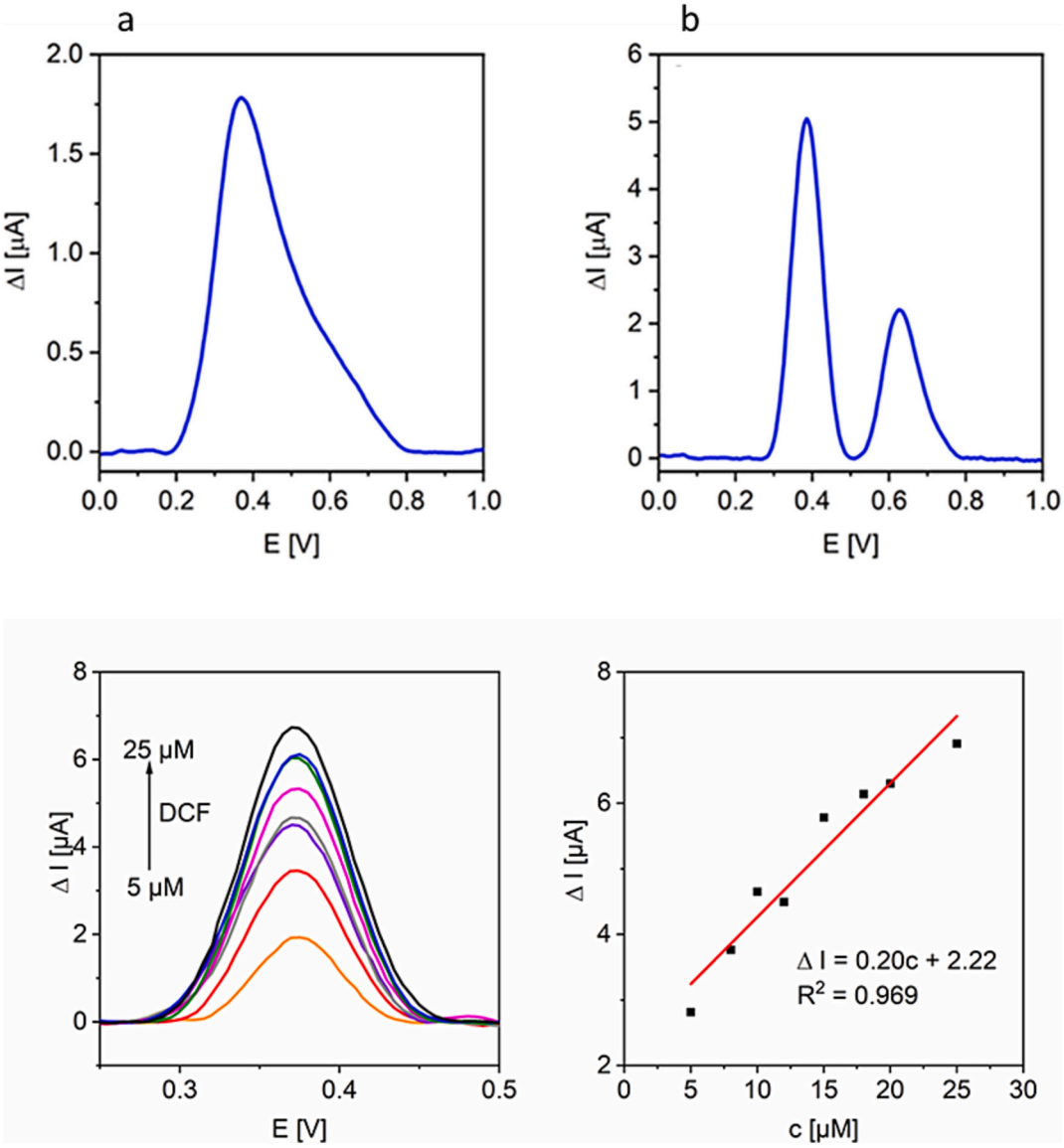

Fig. 7. Baseline corrected DPVs recorded on (a) K/GO-7000_TX_CB_8_TR400 and (b) GCE/TRGO-400 in 0.1 M PBS solution (pH 7.0) containing 100 μM DCF. Baseline-corrected DPVs recorded on GCE modified with TRGO-400 in 0.1 M PBS solution (pH 7.0) containing increasing DCF concentrations (c) and related calibration curve (d).

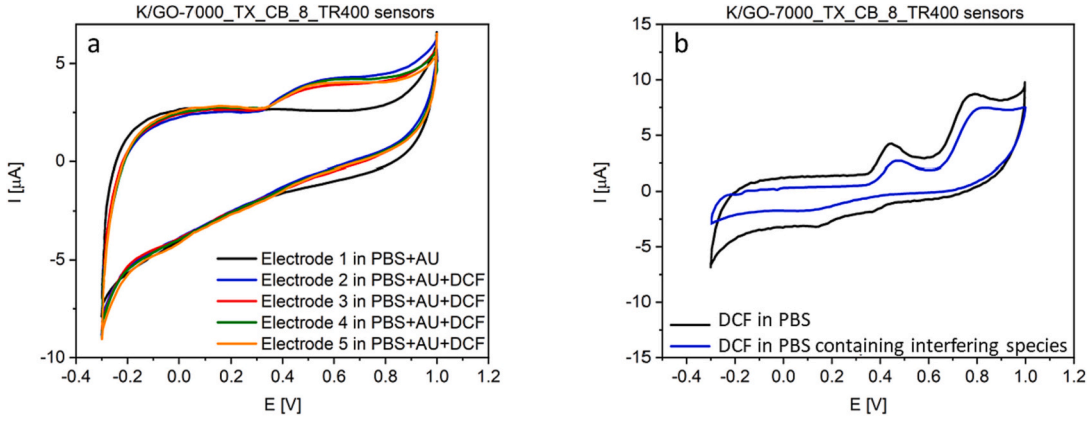

Fig. 8. CVs recorded on (a) K/GO-7000_TX_CB_8_TR400 sensors in a 0.1 M PBS solution (pH 7.0) containing 100 μM DCF and artificial urine (AU) as electrolyte and (b) in presence of common interfering species (K^+, Na^+, Mg^+, SO_4^-, Cl^-, ascorbic acid).

offer a new direction to further investigation.

3.2.3. Preliminary test in real samples, interference studies and reproducibility

Fig. 8 presents the results obtained for preliminary tests in an artificial urine solution and interference studies in the presence of common interfering ions and species. Thus, related measurements were performed in a solution containing 100 μM of DCF and 50 μM of K^+, Na^+, Mg^{2+}, SO_4^-, Cl^-, ascorbic acid and glucose [27,28]. As expected, no peaks are visible in PBS solution only containing artificial urine (Fig. 8a). After addition of 100 μM of DCF a broad anodic peak appears, starting at a potential value close to 0.3 V, which could be explained considering small interferences originated from compounds presented in the artificial urine sample. Even though the sensor performance in terms of selectivity clearly needs to be improved (through the formulation of more appropriate graphene-based inks, as previously mentioned), the developed peak exhibits high current intensity indicating the promising potential of as-proposed IPEs in commercial applications. Moreover, four different K/GO-7000_TX_CB_8_TR400 electrodes were tested. As it can be seen, the electrochemical response recorded on all these electrodes in the 0.1 M PBS solution (pH 7.0) containing artificial urine and DCF is comparable, corroborating the high reproducibility of the proposed electrodes (calculated RSD value close to 3.0 %). Moreover, to assess the reproducibility of electrodes preparation, images showing seven printed K/GO-7000_TX_CB_8_TR400 electrodes are placed in Supporting Information (Fig. S1), revealing the formation of homogenous films on Kapton® as substrate. Moreover, the electrical resistance of those printed layers was measured (Table S1). The obtained resistance values (7.2 to 8.3 kΩ, RSD 5.1 %) are in agreement with homogeneous and reproducible printed sensing platforms. As additional probe reproducibility tests were also performed on three different K/GO-7000_TX_CB_8_TR400 electrodes in the 0.1 M PBS solution containing 100 μM DCF, being the obtained results satisfactory (RSD = 1.3 %). Regarding the impact of interfering compounds (Fig. 8b), it can be seen that not only the capacitive current decreases but also anodic peak ascribed to non-direct DCF sensing. However, a 74 % of the anodic current measured when only DCF is the electroactive specie existing in the solution is maintained. On the other hand, peaks are shifted towards slightly higher overpotentials, which can be the result of a slower electron transfer as a result of undesired adsorption of interfering species on the electrode surface. Nevertheless, both tests (in the real sample and in presence of interferences) shows the high potential of proposed IPEs.

4. Conclusions

In this paper, the promising electrochemical performance of novel, easy to prepare, miniaturized and disposable graphene-based IPEs for DCF sensing was shown and compared to conventionally used modified GCE. Ink formulation was studied, adjusted and optimised in terms of GO concentration, surfactant and conductive additive, along with a range of experimental parameters (design of active pattern and selection of suitable amount of printed GO-based layers). Subsequent thermal treatment (400 °C, 1 h, inert atmosphere) guaranteed the reduction of starting GO material (comparable to that for TRGO-400 powder from thermal exfoliation/reduction of graphite oxide). The resulting active material showed improved characteristics, such as electrical conductivity and type/distribution of oxygenated functional groups. Accordingly, the performance of manufactured IPEs for DCF sensing demonstrate the potential of this novel platform to easily fabricate disposable electrochemical sensors and therefore widen the scope of this kind of sensors for different water contaminants of emerging concern.

CRediT authorship contribution statement

Daria Minta: Conceptualization, Methodology, Investigation, Writing – original draft. **Zoraida González:** Conceptualization, Methodology, Supervision, Writing – review & editing. **Sonia Melendi-Espina:** Methodology, Writing – review & editing. **Grażyna Gryglewicz:** Conceptualization, Methodology, Supervision, Writing – review & editing.

Declaration of competing interest

The authors declare that they have no known competing financial interests or personal relationships that could have appeared to influence the work reported in this paper.

Data availability

Data will be made available on request.

Acknowledgment

Following research was financially supported by a statutory activity subsidy from the Polish Ministry of Science and Higher Education for the Faculty of Chemistry of Wrocław University of Science and Technology.

Appendix A. Supplementary data

Supplementary data to this article can be found online at https://doi.org/10.1016/j.porgcoat.2023.107942.

References

[1] N. Vieno, M. Sillanpää, Fate of diclofenac in municipal wastewater treatment plant - a review, Environ. Int. 69 (2014) 28–39, https://doi.org/10.1016/j.envint.2014.03.021.
[2] W. Boumya, N. Taoufik, M. Achak, H. Bessbousse, A. Elhalil, N. Barka, Electrochemical sensors and biosensors for the determination of diclofenac in pharmaceutical, biological and water samples, Talanta Open 3 (2021), https://doi.org/10.1016/j.talo.2020.100026.
[3] S. Sauvé, M. Desrosiers, A Review of What Is an Emerging Contaminant. http://journal.chemistrycentral.com/content/8/1/15, 2014.
[4] S. Kim, K.H. Chu, Y.A.J. Al-Hamadani, C.M. Park, M. Jang, D.H. Kim, M. Yu, J. Heo, Y. Yoon, Removal of contaminants of emerging concern by membranes in water and wastewater: a review, Chem. Eng. J. 335 (2018) 896–914, https://doi.org/10.1016/j.cej.2017.11.044.
[5] J. Liu, L. Sun, G. Li, J. Hu, Q. He, Ultrasensitive detection of dopamine via electrochemical route on spindle-like α-Fe_2O_3 Mesocrystals/rGO modified GCE, Mater. Res. Bull. 133 (2021), https://doi.org/10.1016/j.materresbull.2020.111050.
[6] B. Wu, L. Xiao, M. Zhang, C. Yang, Q. Li, G. Li, Q. He, J. Liu, Facile synthesis of dendritic-like CeO2/rGO composite and application for detection of uric acid and tryptophan simultaneously, J. Solid State Chem. 296 (2021), https://doi.org/10.1016/j.jssc.2021.122023.
[7] A.J. Bard, L.R. Faulkner, Electrochemical Methods: Fundamentals and Applications, New York, John Wiley & Sons, 2001.
[8] A.K. Geim, K.S. Novoselov, The rise of graphene, Nature 6 (2007) 183–191, https://doi.org/10.1038/nmat1849.
[9] K. Jackowska, P. Krysinski, New trends in the electrochemical sensing of dopamine, Anal. Bioanal. Chem. 405 (2013) 3753–3771, https://doi.org/10.1007/s00216-012-6578-2.
[10] X. Wang, M. Zhang, L. Zhang, J. Xu, X. Xiao, X. Zhang, Inkjet-printed flexible sensors: from function materials, manufacture process, and applications perspective, Mater. Today Commun. 31 (2022), https://doi.org/10.1016/j.mtcomm.2022.103263.
[11] T. Pandhi, C. Cornwell, K. Fujimoto, P. Barnes, J. Cox, H. Xiong, P.H. Davis, H. Subbaraman, J.E. Koehne, D. Estrada, Fully inkjet-printed multilayered graphene-based flexible electrodes for repeatable electrochemical response, RSC Adv. 10 (2020) 38205–38219, https://doi.org/10.1039/d0ra04786d.
[12] C. Karuwan, C. Sriprachuabwong, A. Wisitsoraat, D. Phokharatkul, P. Sritongkham, A. Tuantranont, Inkjet-printed graphene-poly(3,4-ethylenedioxythiophene):poly (styrene- sulfonate) modified on screen printed carbon electrode for electrochemical sensing of salbutamol, Sensors Actuators B Chem. 161 (2012) 549–555, https://doi.org/10.1016/j.snb.2011.10.074.
[13] D. Deng, S. Feng, M. Shi, C. Huang, In situ preparation of silver nanoparticles decorated graphene conductive ink for inkjet printing, J. Mater. Sci. Mater. Electron. 28 (2017) 15411–15417, https://doi.org/10.1007/s10854-017-7427-z.
[14] W.S. Hummers, R.E. Offeman, Preparation of graphitic oxide, J. Am. Chem. Soc. 6 (1958) 1339, https://doi.org/10.1021/ja01539a017.
[15] Z. González, C. Botas, P. Álvarez, S. Roldán, C. Blanco, R. Santamaría, M. Granda, R. Menéndez, Thermally reduced graphite oxide as positive electrode in vanadium

redox flow batteries, Carbon N Y. 50 (2012) 828–834, https://doi.org/10.1016/j.carbon.2011.09.041.
[16] S. Chutipongtanate, V. Thongboonkerd, Systematic comparisons of artificial urine formulas for in vitro cellular study, Anal. Biochem. 402 (2010) 110–112, https://doi.org/10.1016/j.ab.2010.03.031.
[17] L.B. Valdes, Resistivity measurements on germanium for transistors, Proc. IRE 42 (1954) 420–427, https://doi.org/10.1109/JRPROC.1954.274680.
[18] F.M. Smits, Measurement the of sheet resistivities four-point probe, BSTJ. 37 (1958) 711–718, https://doi.org/10.1002/j.1538-7305.1958.tb03883.x.
[19] G. Goos, J. Hartmanis, J. Van, L.E. Board, D. Hutchison, T. Kanade, J. Kittler, J. M. Kleinberg, A. Kobsa, F. Mattern, E. Zurich, J.C. Mitchell, M. Naor, O. Nierstrasz, B. Steffen, M. Sudan, D. Terzopoulos, D. Tygar, G. Weikum, Automatic Morphological Categorisation of Carbon Black Nano-aggregates, 2010.
[20] G. Goos, J. Hartmanis, J. Van, L.E. Board, D. Hutchison, T. Kanade, J. Kittler, J. M. Kleinberg, A. Kobsa, F. Mattern, E. Zurich, J.C. Mitchell, M. Naor, O. Nierstrasz, B. Steffen, M. Sudan, D. Terzopoulos, D. Tygar, G. Weikum, Automatic Morphological Categorisation of Carbon Black Nano-aggregates, International Conference on Database and Epert Sysntems Applications, 2010.
[21] A. Celzard, J.F. Mareche, G. Furdin, F. Furdin, Surface area of compressed expanded graphite, Carbon 40 (2002) 2713–2718, https://doi.org/10.1016/S0008-6223(02)00183-5.
[22] N. Díez, A. Śliwak, S. Gryglewicz, B. Grzyb, G. Gryglewicz, Enhanced reduction of graphene oxide by high-pressure hydrothermal treatment, RSC Adv. 5 (2015) 81831–81837, https://doi.org/10.1039/c5ra14461b.
[23] I. Sengupta, S. Chakraborty, M. Talukdar, S.K. Pal, S. Chakraborty, Thermal reduction of graphene oxide: how temperature influences purity, J. Mater. Res. 33 (2018) 4113–4122, https://doi.org/10.1557/jmr.2018.338.
[24] E. Aliyev, V. Filiz, M.M. Khan, Y.J. Lee, C. Abetz, V. Abetz, Structural characterization of graphene oxide: surface functional groups and fractionated oxidative debris, Nanomaterials 9 (2019), https://doi.org/10.3390/nano9081180.
[25] H. Zhao, D. Zhao, J. Ye, P. Wang, M. Chai, Z. Li, Directional oxygen functionalization by defect in different metamorphic-grade coal-derived carbon materials for sodium storage, Energy Environ. Mater. 5 (2022) 313–320, https://doi.org/10.1002/eem2.12178.
[26] G.Y. Aguilar-Lira, G.A. Álvarez-Romero, A. Zamora-Suárez, M. Palomar-Pardavé, A. Rojas-Hernández, J.A. Rodríguez-Ávila, M.E. Páez-Hernández, New insights on diclofenac electrochemistry using graphite as working electrode, J. Electroanal. Chem. 794 (2017) 182–188, https://doi.org/10.1016/j.jelechem.2017.03.050.
[27] E.M. Almbrok, N.A. Yusof, J. Abdullah, R.M. Zawawi, Electrochemical behavior and detection of diclofenac at a microporous Si_3N_4 membrane modified water-1,6-dichlorohexane interface system, Chemosensors 8 (2020), https://doi.org/10.3390/chemosensors8010011.
[28] S.S.M. Hassan, W.H. Mahmoud, M.A.F. Elmosallamy, M.H. Almarzooqi, S.S. M. Hassan, Determination of diclofenac in pharmaceutical preparations using a novel PVC membrane sensor, Pharmazie 58 (2003).